Clays Clay Miner., Vol. 70, No. 2:252–269, 2022
https://doi.org/10.1007/s42860-022-00181-w

ORIGINAL PAPER

Synthesis and Evaluation of Betaine Copolymer Filtrate Reducer for Drilling Mud

Luo Yunxiang · Lin Ling · Yu Wenke · Li Xin · Gu Han

Accepted: 11 March 2022

Abstract High temperature and a large salt content weaken the surface hydration ability of clay particles in drilling fluid, reduce zeta potential, agglomerate clay particles, increase particle size, and destroy the stability of drilling mud. A filtrate reducer is required, therefore, to maintain the zeta potential of the clay, prevent the agglomeration of clay particles, and maintain good performance of the drilling mud at high temperature and high salt content. To prepare temperature- and salt-resistant polymer filtrate reducer, a betaine monomer was synthesized and copolymerized with a conventional monomer. A betaine monomer 3-(dimethyl (4-vinyl benzyl) ammonia) propyl sulfonate (DVBAPS) was synthesized and then used to create a copolymer filtrate reducer. The copolymer filtrate reducer, referred to as PAAAND, was prepared by free radical copolymerization with 2-acrylamide-2-methylpropane sulfonic acid, acrylic acid, N-vinyl pyrrolidone, acrylamide, and DVBAPS. The optimum synthesis conditions were determined by single factor evaluation, and the chemical structure of the PAAAND was confirmed by Fourier-transform infrared spectroscopy and ^{1}H nuclear magnetic resonance spectroscopy. Results from particle-size distribution and zeta-potential measurements showed that PAAAND increased the zeta potential of clay particles and the distribution width of particles size, which served to maintain the stability of the drilling mud under high-temperature and high-salt conditions. The results of scanning electron microscopy showed that PAAAND made the filter cake formed by clay particles smoother and denser, which reduced filtration loss. The reduction in filtrate loss continued even after aging at high temperature, and, thus, PAAAND performed better than commercial products.

Keywords Acrylamide polymer · Bentonite · Filtrate reducer · Salt resistance · Temperature resistance · Zwitterionic polymer

Introduction

Drilling mud is ‘the blood of drilling engineering.’ It plays a key role in protecting the well wall and controlling the pressure during drilling. The main functional components of drilling fluid are high-quality bentonite and drilling fluid polymer additives. Bentonite is a clay ore with montmorillonite as the main component. As the basic material for configuring drilling fluid, bentonite is used widely in the oil drilling industry. Added sodium bentonite into drilling mud reduces water loss, increases viscosity, increases the yield stress of the drilling mud, and enhances the ability to suspend drilling cuttings. Polymeric additives are one of the most important components of drilling fluid and play a decisive role in its performance. Among polymeric additives, a fluid loss

L. Yunxiang · L. Ling (✉) · Y. Wenke · G. Han
School of Chemistry and Chemical Engineering, Southwest Petroleum University, Chengdu 610500 Sichuan, China
e-mail: cowbolinling@aliyun.com

L. Xin
Petroleum Engineering School, Southwest Petroleum University, Chengdu 610500 Sichuan, China

reducer is considered as the key additive in the water-based drilling fluid (Lee & Tsai, 1994; Liaw & Lin, 1990; Yang, 1998). Up to now, water-based drilling fluids have contained water-soluble polymers as the fluid-loss additive; examples are natural polymers or modified natural polymers such as xanthan gum (De Monaco Lopes et al., 2015), guar gum (Hasan et al., 2018; Sharma et al., 2018), polyanionic cellulose (Liu et al., 2021; Shen et al., 2020; Yang et al., 2015), and sodium carboxymethyl cellulose (Abu-Jdayil & Ghannam, 2014; Murodov et al., 2012).

High temperature and high salinity lead to degradation, dehydration, and other adverse effects of bentonite and polymeric additives (Gurkaynak et al., 1996; Lin et al., 2009; Roux et al., 1973; Xiong et al., 2018; Yang, 1998), which seriously affects the rheological properties of drilling fluid, worsens the wall-building property of drilling fluid, increases the filtration loss, and the safety risk of drilling engineering. Polymeric additives have strong pertinence, outstanding effects on temperature and salt resistance, and are used commonly to protect the colloidal properties of clay in drilling engineering (Lin & Luo, 2015; Ma et al., 2016; Mao et al., 2015; Xiping et al., 2017). A large number of ternary or quaternary copolymers have been synthesized with 2-acrylamide-2-methylpropane sulfonic acid (AMPS) as the main polymerization monomer, by which good temperature and salt resistance has been obtained (Dai et al., 2019; Shen et al., 2020; Tang et al., 2016; Zheng et al., 2013).

In the mid-to-late 1980s, the research and development of water-based drilling-fluid loss additives entered a new phase. Under the research and application of polymer synthesis in combination with 2-acrylamide-2-methylpropane sulfonic acid (AMPS), acrylamide (AM) and alkyl acrylamide (AA), etc., a series of filtrate reducers was synthesized, e.g. COP-1 (AMPS/AM), COP-2 (AMPS/AM) (Perricone et al., 1986), Polydrill, Driscal-D (Zheng et al., 2020), and Dristemp, etc. These polymer additives can endure high temperatures and high concentrations of salt, including calcium. However, due to the high cost of synthesizing these polymers, their application is still limited. In recent years, to develop excellent filtrate reducers, more monomers were synthesized and used for synthesizing copolymers (Liu et al., 2018; Liu et al., 2019; Wang et al., 2020). All of these studies promoted the development of artificially synthesized polymer fluid-loss agents.

Most recently, Li et al. (2014) used acrylamide (AM), 2-acrylamide-2-methylpropane sulfonic acid, sodium styrene sulfonate (SSS), and N-vinyl pyrrolidone (NVP) monomers with redox initiators to synthesize a quaternary copolymer filtration controller which performs well at temperatures up to 200°C. Zhao et al. (2015) used N, N-dimethyl acrylamide (DMAA), 2-acrylamide-2-methyl-1-propyl (AMPS), dimethyl diallyl ammonium chloride (DMDAAC), and N-vinyl pyrrolidone (NVP) to synthesize a zwitterionic copolymer via free radical copolymerization, which could control the fluid loss of drilling fluid under 220°C and saturated NaCl conditions. Chang et al. (2020) used 4-vinyl pyridine (VP), N,N-dimethyl acrylamide (DMAA), 2-acrylamide-2-methylpropane sulfonic acid, and N-vinyl caprolactam (NVCL) to synthesize a zwitterionic copolymer filtrate reducer, PDANV, through free radical copolymerization. The fluid loss (FL_{API}) of PDANV in WBDFs was only 3.4 and 6.0 mL, before and after aging at 260°C for 16 h. However, two monomers are too expensive for industrial production. Mao et al. (2020) prepared an anionic filtrate reducer P(ANAN) using 2-acrylamide-2-methylpropane sulfonic acid (AMPS), N-vinyl-2-pyrrolidone (NVP), and acrylamide (AM). The fluid-loss tests show that P(ANAN) can resist a compound salt solution containing 4.5×10^5 ppm of Cl^-, 4×10^5 ppm of Ca^{2+}, and 1.5×10^4 ppm of Mg^{2+} at 180°C.

The main goal of the preparation of a copolymer filtrate reducer is to introduce sulfonic acid monomer, a rigid group, a hydrophobic monomer, and a cationic monomer to prepare the temperature and salt-resistant copolymer filtrate reducer. Some researchers also choose nanocomposites to improve the performance of the filtrate reducer.

The goal of the current study was to improve the performance of drilling muds under conditions of high temperature and high salt content by amending the constituent bentonite with a newly synthesized copolymer, PAAAND, consisting of DVBAPS combined with the monomers AM, AA, AMPS, and NVP. The hypothesis was that this newly synthesized copolymer would protect the clay particles in the drilling mud by preventing changes in zeta potential and particle size.

Materials and Method

Materials

Sodium hydroxide, acrylamide (AM), N-vinyl pyrrolidone (NVP), acrylamide, ammonium persulfate, petroleum ether, 4-vinyl benzyl chloride, 1,3-propane sulfonic

https://doi.org/10.1007/s42860-022-00181-w Published online by Cambridge University Press

acid lactone, potassium carbonate, dimethylamine (AR, Adama's beta); sodium bisulfite, ethanol, and acetonitrile (AR) were obtained from Chengdu Kelong Chemical Reagent Factory (Chengdu, China). Bentonite was obtained from Hualai Dingsheng Company (Shijiazhuang, China). The main component of bentonite is montmorillonite and was used directly without treatment.

Synthesis of DVBAPS

Potassium carbonate (55.3 g, 0.4 mol) was dissolved in a flask containing 200 mL of anhydrous ethanol equipped with a thermometer, a dropping funnel, and a magnetic stirrer. Then, a nitrogen inlet and 4-vinylbenzyl chloride (30.5 g, 0.2 mol) and dimethylamine solution (20 mL, 0.9 g/mL) were added to the flask in a drop-wise manner, and the reaction mixture was heated to 50°C and stirred for 24 h (Xiao et al., 2018).

Subsequently, the solvent was evaporated and purified by column chromatography using petroleum ether as a solvent, and distilled under vacuum to get a light yellow transparent oily liquid of N,N-dimethyl-vinyl benzylamine. Then, N,N-dimethyl-vinyl benzylamine (3.22 g, 20 mmol) and 1,3-propane sultone (2.44 g, 20 mmol) were added and dissolved in 100 mL dry acetonitrile in a 250 mL flask; the reaction was carried out at 50°C under stirring for 12 h. The white precipitate produced was recovered through filtration. The precipitate was then dried in a vacuum oven at 50°C and stored at 0 to 8°C. The synthesis mechanism is shown in Fig. 1. The nucleophilic substitution reaction between vinyl benzyl chloride and dimethylamine produces an intermediate product which reacts with 1,3-propane sulfonic acid lactone to form an internal salt and precipitate from the solvent. The products were tested by Fourier-transform infrared (FTIR) spectroscopy and ^{1}H nuclear magnetic resonance (NMR) spectroscopy.

Synthesis of Copolymer PAAAND

Polymers were synthesized by free radical aqueous solution copolymerization. Known amounts of AA, AM, and AMPS were dissolved in an aqueous solution; NaOH solution (1.0 mol/L) was used to adjust the pH, then the prepared solution was transferred to a four-necked flask. NVP and DVBAPS were added and the solution was stirred for 5 min. Nitrogen was used to degas the oxygen, a certain amount of initiator was added, and the product was taken out after reaction at constant temperature for a certain time. The product was then rinsed with absolute ethanol, cut into pieces and granulated, and dried to obtain a copolymer sample for standby. The synthesis mechanism of the copolymer, P(AM/AA/AMPS/NVP/DVBAPS) named PAAAND, is shown in Fig. 2. The five monomers were initiated by V50 to form active free radicals and then random copolymerization of free radicals occurred.

Characterization

A Bruker-AC-E200 nuclear magnetic analyzer (Bruker, Switzerland) was used for the nuclear magnetic resonance spectroscopy test. The ^{1}H spectrum of PAAAND was scanned using deuterated water (D_2O) as solvent. The thermal stability of the PAAAND in nitrogen was tested using the STA449F3 synchronous thermal analyzer (NETZSCH-Gerätebau GmbH, Germany). The tested temperature ranged from 35 to 800°C; the heating rate was 10°C/min.

The infrared spectrum of PAAAND was collected using a Nicolet 6700 spectrophotometer (Thermo Scientific, Madison, Wisconsin, USA) over the range 4000–500 cm^{-1}. The molecular weight of the polymer was tested by GPC-20A gel chromatography

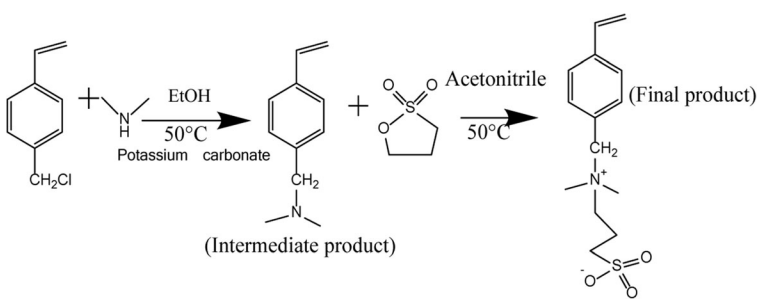

Fig. 1 Synthesis mechanism of DVBAPS

https://doi.org/10.1007/s42860-022-00181-w Published online by Cambridge University Press

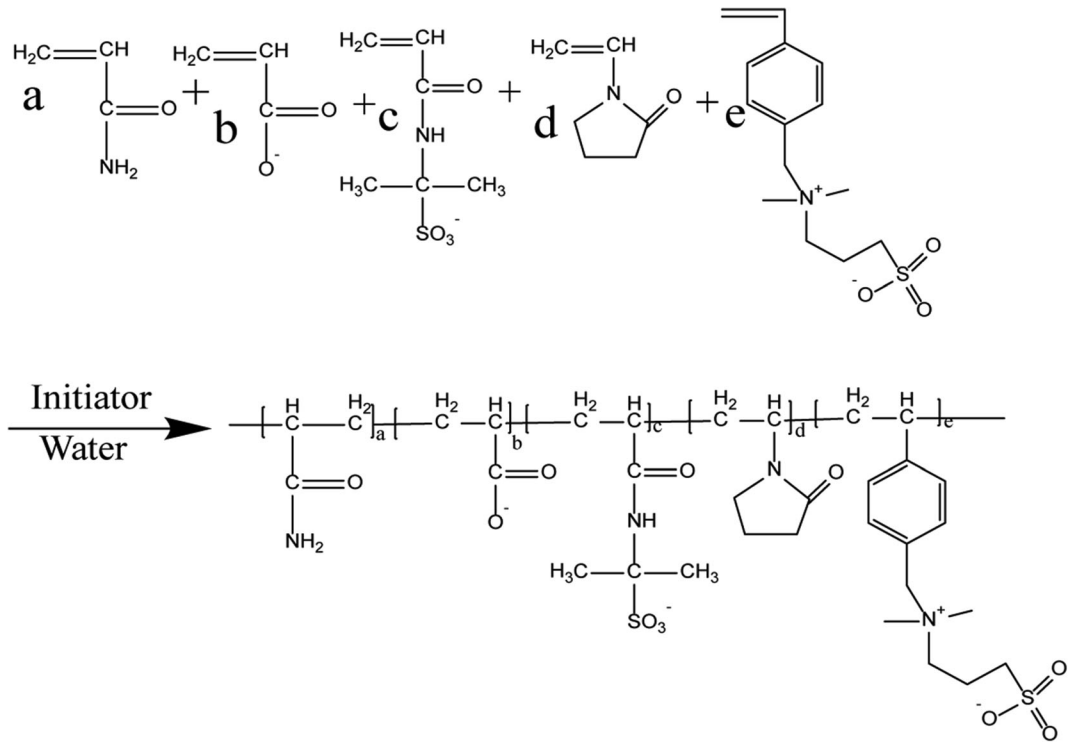

Fig. 2 Synthesis mechanism of the copolymer

(Shimadzu, Shimane Prefecture, Japan) with water as the mobile phase.

Performance Evaluation of PAAAND with Aging Treatment

A base slurry was obtained by mixing 40 g bentonite in 1000 mL of distilled water at 11,000 rpm (2000×*g*) for 20 min, then aged at room temperature for 24 h.

PAAAND was added to the base slurry and aged under room temperature for 16 h, then the API filtration was tested. The drilling fluid was heated at a high temperature (≥200°C) for 16 h. After cooling, the API filtration was tested. Two parameters obtained were FL_{API}, which is the recorded filtration within 30 min at room temperature and 0.69 MPa, and FL_{HTHP}, which is the recorded filtration within 30 min at 160°C and 3.5 MPa. The filtration loss, FL_{HTHP}, was then multiplied by 2. The microstructure of the API filter cake was observed by by means of SEM. The particle-size distribution of the drilling fluid before and after aging was tested with a Mastersizer 2000 laser particle size analyzer (Malvern Panalytical, Malvern, UK).

Results and Discussion

Characterization and Testing

Characterization of DVBAPS The infrared spectrum of DVBAPS is given in Fig. 3a. The absorption peaks were assigned as follows: 3450 cm^{-1}, the stretching vibration of residual dimethylamine amino groups; 3020 cm^{-1}, the vinyl C-H absorption; 2920 cm^{-1}, the methyl and methylene absorption; 1636 cm^{-1}, the C=C double bond stretching vibration; 1482 cm^{-1}, the asymmetric bending of methyl; 1188, 1068, and 620 cm^{-1}, the characteristic bands of the sulfonic acid group; and 840 cm^{-1}, characteristic of the p-disubstituted benzene ring. Chemical shifts in the ^{1}H NMR of DVBAPS (Fig. 3c) were: δ 7.60 and δ 7.49 corresponding to H on a benzene ring; δ 6.82, 5.94, and 5.41 were introduced by H on vinyl groups; δ 4.47, 3.43, 2.96, and 2.31 are the corresponding methylene on the monomer; and δ 3.03 corresponds to two methyl groups. The monomer DVBAPS was synthesized successfully, as demonstrated by both FTIR and ^{1}H NMR spectra (Yuan et al., 2021).

https://doi.org/10.1007/s42860-022-00181-w Published online by Cambridge University Press

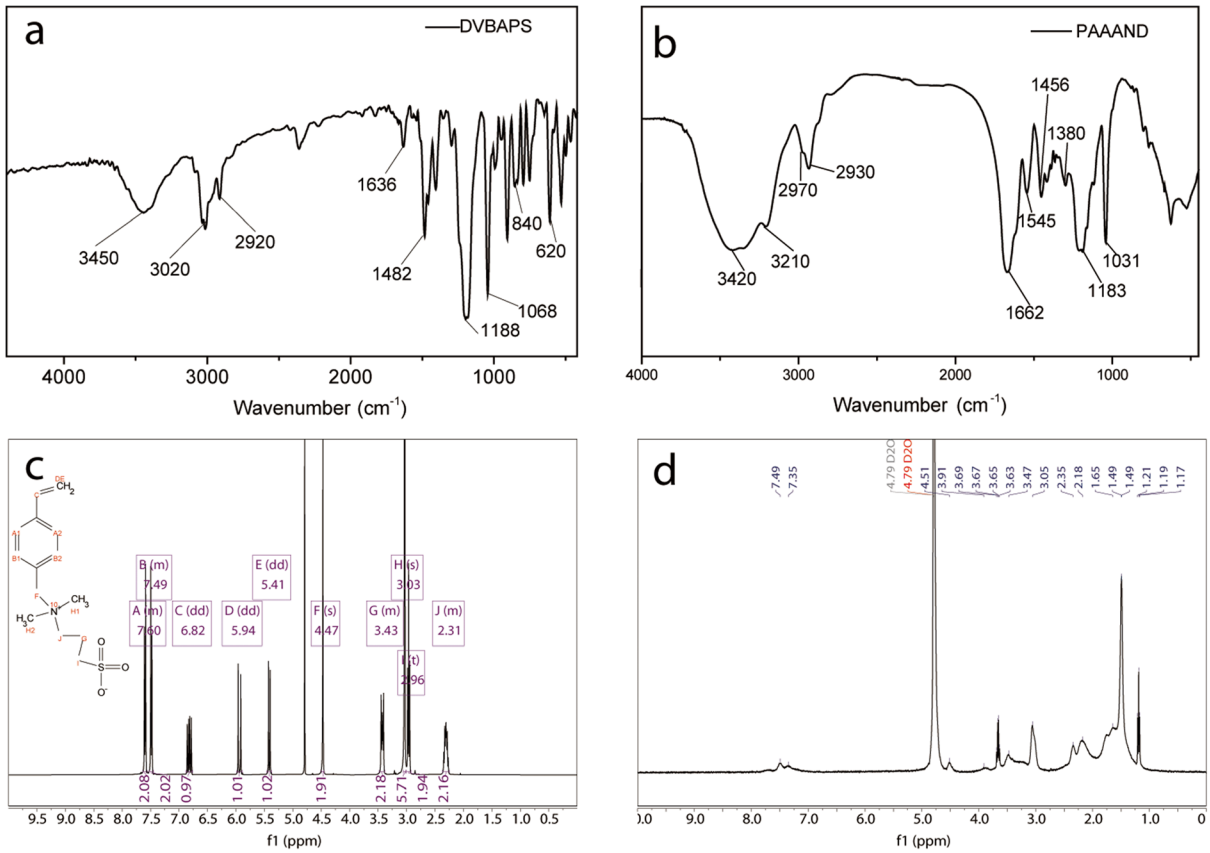

Fig. 3 **a** The infrared spectrum of DVBAPS, **b** the infrared spectrum of PAAAND, **c** the ^{1}H NMR spectrum of DVBAPS, and **d** the ^{1}H NMR spectrum of PAAAND

Characterization of PAAAND The infrared spectrum of P AAAND is given in Fig. 3b. The band at 3420 cm^{-1} is the amino stretching vibration; the bands at 2970 and 2930 cm^{-1} are methyl methylene absorption; the band at 1662 cm^{-1} is the carbonyl -C=O absorption; the band at 1456 cm^{-1} is the asymmetric bending of methyl; the band at 1545 cm^{-1} is the corresponding characteristic absorption of a benzene ring; the bands at 1183, 1031, and 621 cm^{-1} are the corresponding absorption by sulfonic acid groups.

The ^{1}H NMR spectrum of the copolymer is given in Fig. 3d. The chemical shifts δ 7.49 and 7.35 correspond to a benzene ring; δ 1.37–1.55, to the methylene on the polymer; δ 2.18, to methylene on the NVP ring; and δ 3.57, to the corresponding methyl on AMPS and DVBAPS monomers in polymerization. No double bond peak was observed in the NMR spectrum. Therefore, ^{1}H NMR and FTIR showed that PAAAND copolymer was prepared successfully (Li et al., 2012; Zheng et al., 2021).

Thermal analysis (TG-DTG) of PAAAND The TG-DTG of PAAAND (Fig. 4) revealed that the first DTG peak was at 97°C, and the TG curve showed that the mass decreased by 15.8% at 35–313°C, which was

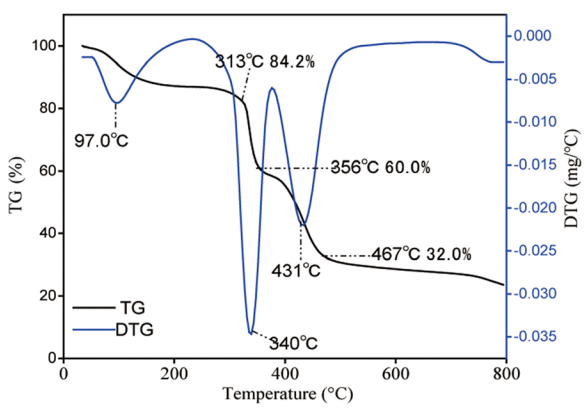

Fig. 4 Thermal analysis (TG-DTG) of PAAAND

https://doi.org/10.1007/s42860-022-00181-w Published online by Cambridge University Press

the mass loss of residual solvents (water and ethanol) in the polymer and the mass loss of amido amidation in the polymer. Above 313°C, two DTG peaks corresponded to the side chain decarboxylation degradation and main chain fracture of the polymer, respectively. The first DTG peak appeared at 340°C, which showed that the copolymer had good temperature resistance.

Molecular weight of PAAAND At the present time, polymer treatment agents used in drilling mud are mostly high-molecular-weight water-soluble polymers with molecular weights ranging from millions to tens of millions. When the molecular weight of the polymer treatment agent is too large, it will lead to excessive viscosity of the drilling mud and poor rheological properties. However, when the molecular weight of the polymer treatment agent is small, it often has poor temperature resistance and no filtration reduction effect. The average molecular weight obtained from the GPC test of copolymer filtrate reducer PAAAND (Table 1) was 5×10^4, which can increase viscosity and reduce filtrate loss.

Optimization of Synthesis Conditions for PAAAND

The single factor experiment was used to determine the optimal synthesis conditions with the base slurry as the test sample. The mass fraction of PAAAND was 1%, using the API water loss before and after aging as the evaluation standard. The initial synthesis conditions were: reaction temperature 50°C, pH 7.0, monomer concentration 20 wt.%, initiator concentration 0.4 wt.%, aging temperature 200°C, and aging time 16 h.

Effect of AM/AA Monomer Ratio (Fig. 5a) As the backbone of the main chain in the polymer, AM forms a large proportion of the monomer ratio. Increasing the proportion of AM can improve the molecular weight of the polymer. However, a high AM ratio will affect seriously the temperature resistance of the polymer. With n(AMPS):n(NVP):n(DVBAPS) proportions fixed at 20:10:5, the filtration reduction effect of various n(AM):n(AA) ratios on the polymer before and after aging in slurry was investigated. With increase of n(AM):n(AA), FL_{API} decreased firstly and then increased. When n(AM):n (AA) proportions were 30:25, the FL_{API} before aging was at its smallest, and the FL_{API} after aging was also its smallest. When the proportion of AM was large, the relative molecular weight of the polymer also increased, but the decrease of the carboxyl group reduced the negative charge on the surface of clay particles and the repulsion between clay particles, which made particle coalescence easy and enabled small particles to become large particles, thus increasing filtration. A value of n(AM):n(AA) of 30 : 25 was, therefore, selected.

Table 1 Result of GPC measurement

Distribution type	Mn	Mw	Mz	Mw/Mn
Molecular weight	503,409	795,935	1,421,011	1.58109

Mn: number average molecular weight, Mw: weight average ular weight, Mz: z average molecular weight

Effect of DVBAPS Monomer Ratio (Fig. 5b) The sulfonic acid group has good hydration ability and can enhance the temperature and salt resistance of the polymer. DVBAPS is a monomer containing a sulfonic acid group and a quaternary ammonium cation. Quaternary ammonium cations are conducive to enhancing the adsorption capacity of the polymer on the clay, but too high a cation content will lead to clay mineral flocculation. A fixed n(AM):n(AA):n(AMPS):n(NVP) proportion of 30:25:20:10, was used, therefore, to investigate the effect of the DVBAPS ratio on filtration. When the proportion of DVBAPS was large (≧8), the filtration loss was also large but decreased with decreasing DVBAPS. Large proportions of DVBAPS caused the polymer to form an insoluble gel, which affected the solubility of the polymer. The assumption was that the large amount of quaternary ammonium cation inhibited the dispersion of the clay and increased the filtrate loss. Choosing n(DVBAPS) = 5 is more appropriate.

Effect of AMPS Monomer Ratio (Fig. 5c) AMPS is stable and insensitive to temperature and ions. It is used commonly as a temperature- and salt-resistant monomer. However, the steric hindrance of the AMPS monomer is large. When more AMPS is present, the molecular weight of the polymer is often low, resulting in large filtration loss. Finding an appropriate proportion, such as n(AM):n(AA):n(DVBAPS):n(NVP):n(AMPS) = 30:25:5:10:25, was, therefore, necessary. When

https://doi.org/10.1007/s42860-022-00181-w Published online by Cambridge University Press

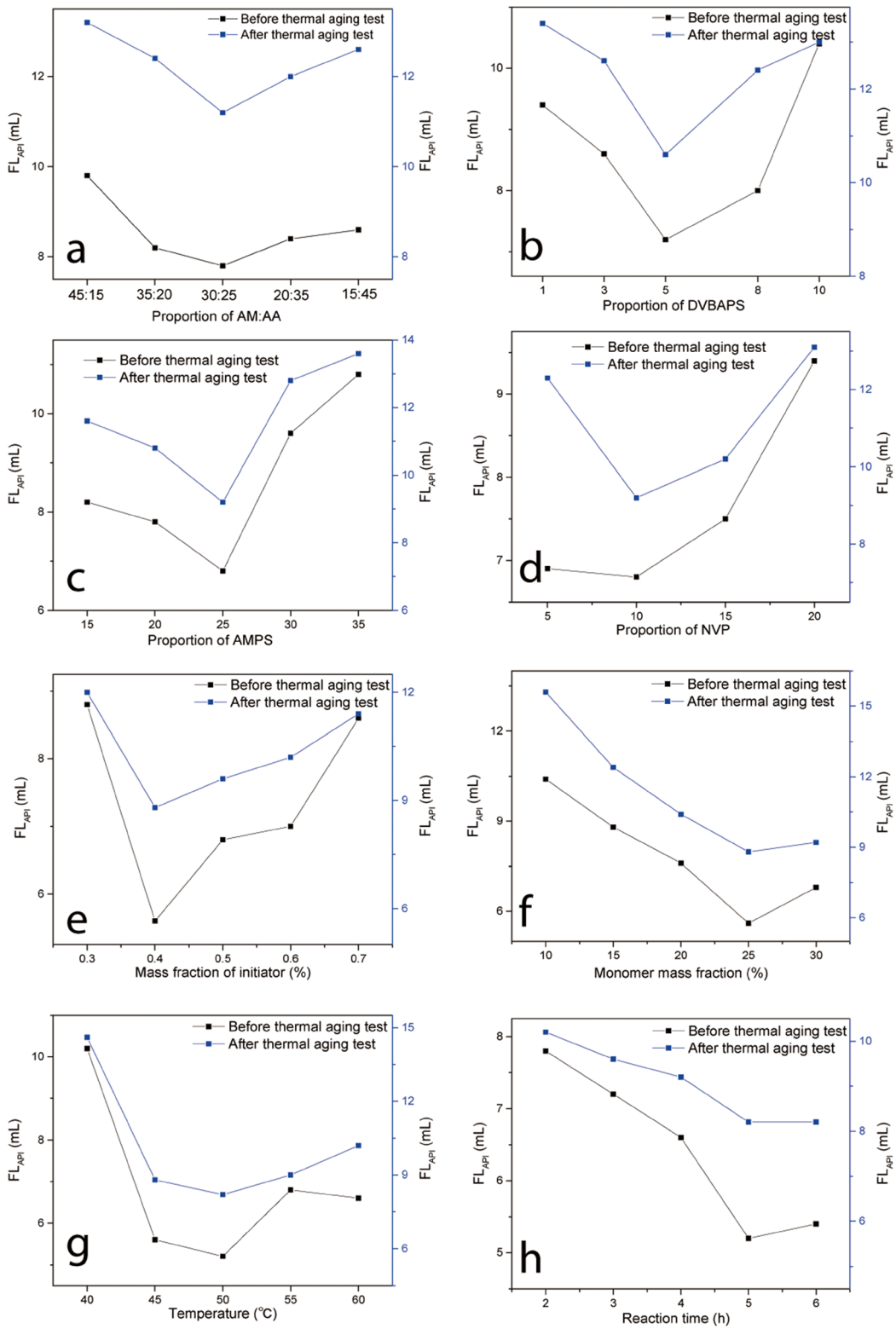

Fig. 5 The effects on filtration of: **a** the ratio AM:AA, **b** DVBAPS proportion, **c** AMPS proportion, **d** NVP proportion, **e** total monomer dosage, **f** initiator ratio, **g** reaction temperature, and **h** reaction time

https://doi.org/10.1007/s42860-022-00181-w Published online by Cambridge University Press

the AMPS dosage was 35, the filtration loss was large. After reducing the proportion to 20, the filtration loss decreased and the optimum level was determined to be 25.

Effect of NVP Monomer Ratio (Fig. 5d) NVP is a rigid monomer, which can improve the temperature resistance of the polymer. The n(AM):n(AA):n(AMPS):n(DVBAPS) proportion was fixed at 30:25:25:5 to investigate the effect of NVP proportion on polymer filtration. When the proportion of NVP was 5, the filtration loss after aging was large. When the proportion of NVP was increased, the filtration loss decreased. When the proportion of NVP was >15, however, the polymer formed an insoluble gel, which increased the filtrate loss of the polymer. The proportion of NVP selected was, therefore, 10.

Effect of Total Monomer Dosage (Fig. 5e) The effect of the total amount of monomer on the filtration reduction performance of polymer PAAAND revealed that as the total amount of monomer increased, the FL_{API} before and after polymer aging first decreased and then increased. This is because when the monomer concentration was low, the polymer molecular weight was small, but when the total amount of monomer continued to increase, the free radical concentration increased and the chain transfer and chain termination rates increased, The relative molecular weight of PAAAND decreased. Therefore, the suitable total amount of monomer selected was 25%.

Effect of Initiator Dosage (Fig. 5f) The change of filtration amount of polymer PAAAND before and after aging under increasing initiator dosages showed that the API filtration before and after aging increased first and then decreased. When the amount of initiator was small, the initiation efficiency was low and the molecular weight of the polymer was low. Excessive addition of the initiator will lead to excessive free radicals and a decrease of polymer molecular weight. Therefore, the effect was believed to be best with the addition of 0.4 wt.% initiator relative to the total mass of the monomer.

Effect of Reaction Temperature (Fig. 5g) The change in FL_{API} with increasing reaction temperature before and after the aging of polymer PAAAND showed that the API filtration before and after aging decreased first and then increased. When the temperature was 50°C, the filtration was lowest. Therefore, the polymerization temperature was set at 50°C.

Effect of Reaction Time (Fig. 5h) When the reaction time was short, the formation of PAAAND was incomplete; the molecular weight of the polymer generated was low, and the filtration loss was large. With increasing reaction time, the molecular weight of the polymer increased and the filtration loss decreased. When the reaction time exceeded 5 h, the change of filtration rate was not obvious, indicating that the reaction had been complete, so a reaction time of 5 h was selected.

PAAAND Filtration Reduction Performance

Effect of PAAAND Dosage The effect of PAAAND dosage on the filtration performance of the base slurry (Table 2) was that the API filtration decreased before and after aging as the PAAAND dosage increased. When the dosage of PAAAND was 0.5 wt.%, the API before aging was 8.6 mL, and the API after aging was 11 mL, indicating that it still had a good filtration reduction effect when the dosage was small. When the dosage reached 2 wt.% by mass, the effect was best. After aging, the API was controlled at 6.8 mL, which had a good filtration-reduction effect. The aging temperature was 200°C and the aging time 16 h.

Temperature Resistance For PAAAND, the effect of base slurry with a mass fraction of 2 wt.% (Table 3) was that FL_{API} tended to increase with increasing aging temperature, whereas FL_{HTHP} was <30 mL at temperatures <230°C, which proved that PAAAND is resistant to temperature changes in that range. The maximum temperature and high-pressure filtration were 160°C and 3.5 MPa, respectively.

Salt Resistance Polymers of various qualities were added to a saturated NaCl-based slurry to investigate their respective salt resistances (Table 4). With increasing amount of polymer, FL_{API} decreased gradually. When the PAAAND

Table 2 Effect of PAAAND dosage on PAAAND filtration

PAAAND dosage (wt.%)	Before aging FL_{API} (mL)	After aging FL_{API} (mL)
0	28	122
0.5	8.6	11
1	5.2	8.2
1.5	5	7.8
2	4.8	6.8

https://doi.org/10.1007/s42860-022-00181-w Published online by Cambridge University Press

Table 3 Effect of aging temperature on PAAAND filtration

Temperature (°C)	After aging FL_{API} (mL)	FL_{HTHP} (mL)
180	6.2	18
200	6.8	20.6
220	7.8	22.2
230	8.4	25.6

dosage was 0.5%, FL_{API} was controlled within 6.2 mL and FL_{HTHP} was controlled within 17.8 mL, which proved that PAAAND can resist saturated NaCl solutions. When the polymer dosage was 2 wt.%, FL_{API} was 3.0 mL and FL_{HTHP} was 14.4 mL. Further increases in the polymer dosage had no obvious effect on filtration. The experimental conditions of high-temperature and high-pressure filtration were 160°C and 3.5 MPa, respectively.

Comparison of Similar Products To verify the filtration-reduction ability of PAAAND, results of filtration tests using a 1 wt.% dose of Driscal-D, Dristemp, and Polydrill were compared (Table 5). Each of the filtration-reduction agents, including PAAAND, was added to the base slurry for API tests before and after aging. The results showed that PAAAND had a good filtration-reduction effect, and its filtration-reduction ability was significantly better than that of Driscal-D, Dristemp, and Polydrill. The aging temperature was 200°C and the aging time was 16 h.

PAAAND Filtration-Reduction Mechanism

Clay-Expansion Inhibition The main component of bentonite is montmorillonite. The crystal structure of montmorillonite is that one Al-O octahedral sheet is sandwiched between two Si-O tetrahedral sheets to form a unit-structure layer. The two adjacent crystal layers are oxygen atoms, and the crystal planes are close to each other. No hydrogen bond exists between the layers, but only van der Waals forces. This connection is relatively weak. When montmorillonite is in an aqueous environment, water and other polar molecules are attracted to the basal surfaces of the crystal layer, showing obvious expansibility. PAAAND was added to the base slurry and dried to obtain the powder, which was then analyzed by XRD and compared with the original clay (Fig. 6). The original bentonite layer spacing was $d_{bentonite}$ = 1.548 nm. After adding PAAAND and aging at 220°C, the layer spacing was $d_{PAAAND/bentonite}$ = 1.226 nm. After adding PAAAND, the spacing of the bentonite layer decreased, which meant that the expansion of the clay layers was restrained.

Table 4 Effect of saturated NaCl-based slurry PAAAND on filtration

PAAAND dosage (wt.%)	Before aging FL_{API} (mL)	FL_{HTHP} (mL)
0	198	all lost
0.5	6.2	17.8
1	3.8	16
1.5	3.2	15.4
2	3	14.4

Table 5 Evaluation of filtrate reducers

Filtrate reducer	Before aging FL_{API} (mL)	After aging FL_{API} (mL)
Driscal-D	13.5	26
Dristemp	8.4	22
Polydrill	15.6	44
PAAAND	5.2	8.2

Particle-size Distribution Test During the filtration of drilling fluid into the formation, it is deposited continuously on the well wall. In this process, the large clay particles form a skeleton and block the pore channels. The smaller particles gradually fill the pores and adhere to the large particles until a dense and smooth filter cake is formed. Formation of a high-quality filter cake

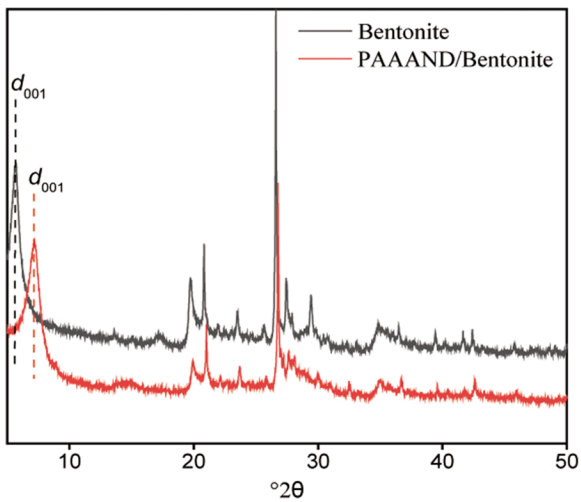

Fig. 6 XRD patterns of bentonite before and after adsorption of PAAAND

https://doi.org/10.1007/s42860-022-00181-w Published online by Cambridge University Press

requires a reasonable size distribution of particles in the drilling fluid system. During drilling, the particle-size distribution of the drilling fluid system is affected by copolymers, electrolytes, high-temperature aging, and other factors. The addition of the copolymer PAAAND at a mass fraction of 0, 0.5, 1, 1.5, or 2 wt.% resulted in the median and average particles size in the system first decreasing and then increasing (Fig. 7) The PAAAND

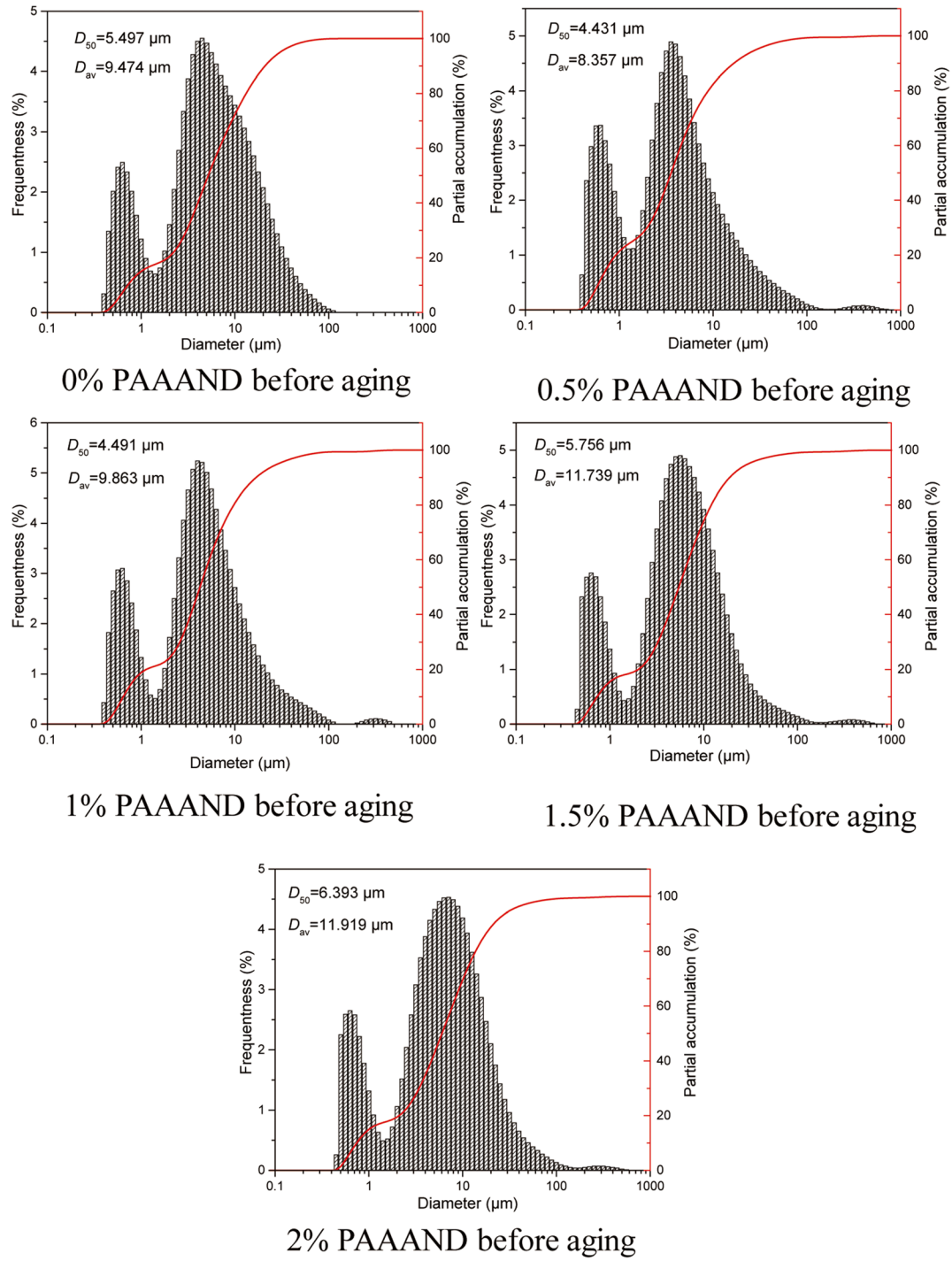

Fig. 7 Particle-size distribution of base slurry before aging with various mass fractions of PAAAND

https://doi.org/10.1007/s42860-022-00181-w Published online by Cambridge University Press

base slurry had a broader particle-size distribution than the zero-PAAAND base slurry. After PAAAND was added, the particle-size distribution changed from bimodal to trimodal. According to the theory of Smith et al. (1996), when the particle-size distribution is large, the porosity and permeability of the filter cake are small. When the mass fraction of PAAAND was <1 wt.%, a layer of polymer with anionic groups became attached to the polymer surface through adsorption, and the particle size of the system was reduced because of electrostatic repulsion. As the dosage of the polymer increased, the amount attached to the clay surfaces increased and the particle size of the system increased.

The particle-size distribution of the base slurry after aging at 230°C for 16 h had a narrower distribution than before aging (Fig. 8). After aging, the particle size of the zero-PAAAND base slurry increased significantly. When the mass fraction of PAAAND was >1 wt.%, the particle size increased slightly. The reason is that the number of polymers increased, and the amount of polymer attached to the clay surfaces also increased, which increased the particle size of the system. The addition of PAAAND made the particle-size distribution of the system wider. The filtration loss was reduced effectively through the interaction between the polymer and the clay and between polymer molecules.

PAAAND can reduce significantly the particle-size distribution of the brine base slurry (Fig. 9). The addition of NaCl collapsed the diffuse double layer of the clay layers, thus enabling them to polymerize. However, after PAAAND was added, the polymer maintained electrostatic repulsion between the clay layers due to the large number of anionic groups, which decreased the particle size so that the fine particles could still maintain a sufficient proportion to ensure the quality of the filter cake.

Filter-cake Macro-Morphology Photographs of the filter cake from 1 wt.% PAAAND before and after aging the base slurry (Fig. 10) allowed for visual inspection of the thickness of the filter cake. The filtration loss of drilling mud is usually related to the thickness of filter cake. The thin filter cake has a small filtration loss and the thick filter cake has a large filtration loss, mainly due to the large permeability of thick filter cakes and small permeability of thin filter cakes. The filter cake of the base slurry before aging is thick and loose. The filter cake of the base slurry after adding 1 wt.% PAAAND but before aging is thin and dense, so it has a good filtration reduction effect. After aging, the filter cake became thicker and the filtration loss increased. After the addition of 1 wt.% PAAAND, the filter cake was still thin and dense after aging. Therefore, PAAAND had a good filtration reduction effect and can improve significantly the morphology of the filter cake. The base slurry filter cake without PAAAND is shown in Fig. 10 for comparison.

Filter-cake Micromorphology The permeability of the filter cake is the main factor affecting the filtration of drilling mud, and can be visualized through the micromorphology revealed by SEM. To reduce the filtration of drilling fluid, improving the compactness of the filter cake and reducing its permeability are necessary. These qualities are achieved with smaller clay particles. SEM results (Fig. 11) from the base slurry filter cake before aging, the 1 wt.% PAAAND base slurry filter cake before aging, and the 1wt.% PAAAND base slurry filter cake after aging found that the surface of base slurry filter cake before aging is rougher than that of the 1 wt.% PAAAND base slurry filter cake before aging, suggesting that the latter contains a more uniform particle-size distribution than the latter. Magnification of the images by 10,000× revealed more folds and gaps on the surface of the former than the latter, providing further evidence for the differences in uniformity. Although the particle distribution of the 1 wt.% PAAAND-based slurry filter cake after aging was not as uniform as that before aging, it was still smoother and more uniform than that before aging base slurry without the copolymer, which strongly indicates that PAAAND can effectively reduce the loss of base slurry before and after aging.

The foregoing analyses suggest that the ionic groups contained in the polymer PAAAND are adsorbed on the surface of the clay particles by electrostatic attraction, hydrogen bonding, and van der Waals forces, which enhance the dispersion of the clay particles. The ability to bridge easily between molecules, along with the adsorption of clay particles, forms a supramolecular grid structure, which increases the viscosity of the PAAAND-based slurry, and at the same time makes coalescence of the clay particles difficult, thus reducing the fluid loss of the PAAAND-f-based slurry.

https://doi.org/10.1007/s42860-022-00181-w Published online by Cambridge University Press

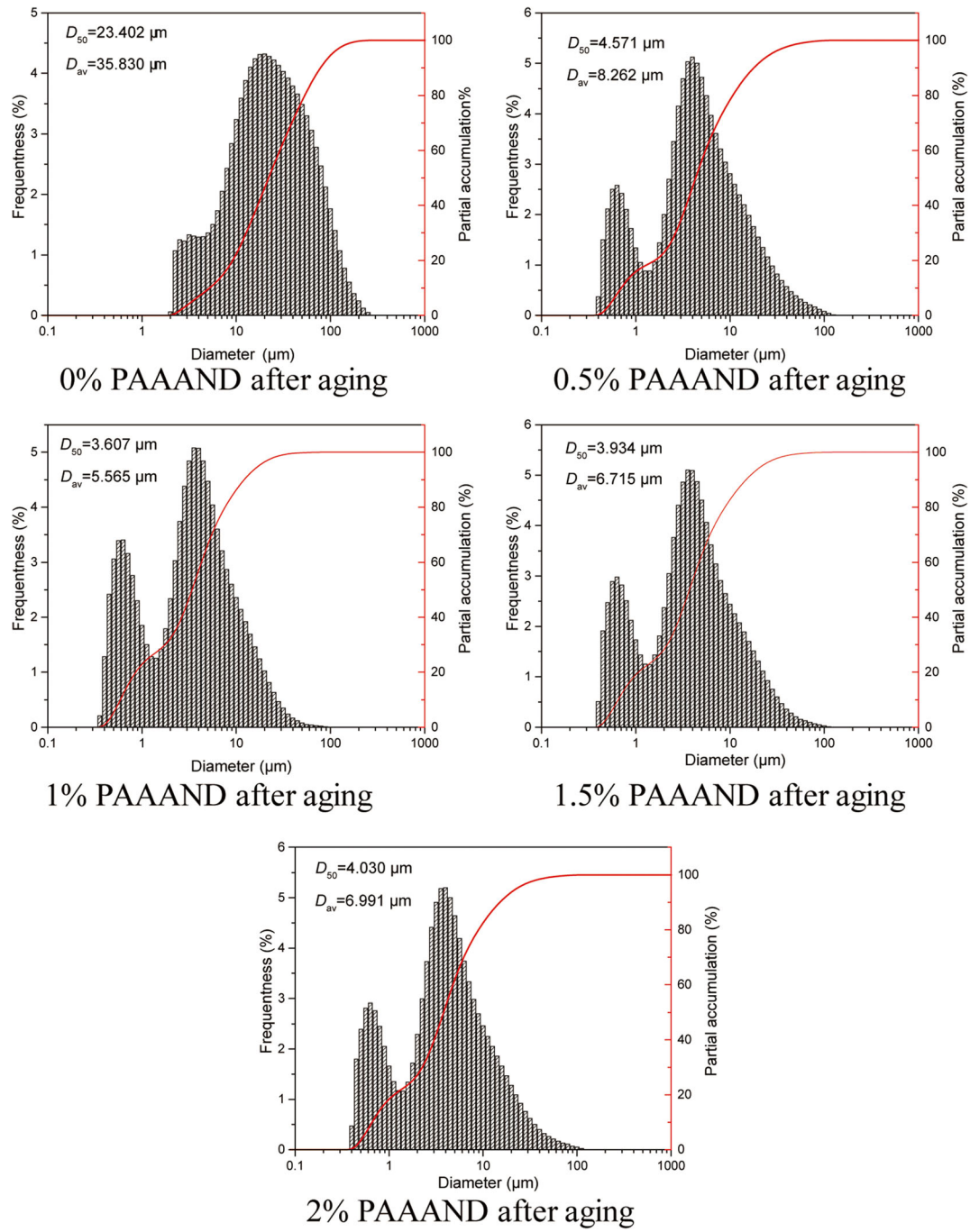

Fig. 8 Particle-size distribution of base slurry after aging with various mass fractions of PAAAND

Zeta Potential

According to DLVO theory (Hermansson, 1999; Pashley & Israelachvili, 1984), zeta potential can reflect accurately the electrostatic repulsion between clay particles and then reflect the colloidal stability of the drilling mud. The absolute value of the zeta potential of the clay particles in the drilling mud increased with increasing PAAAND content (Fig. 12), but decreased after aging, indicating that its colloidal stability

https://doi.org/10.1007/s42860-022-00181-w Published online by Cambridge University Press

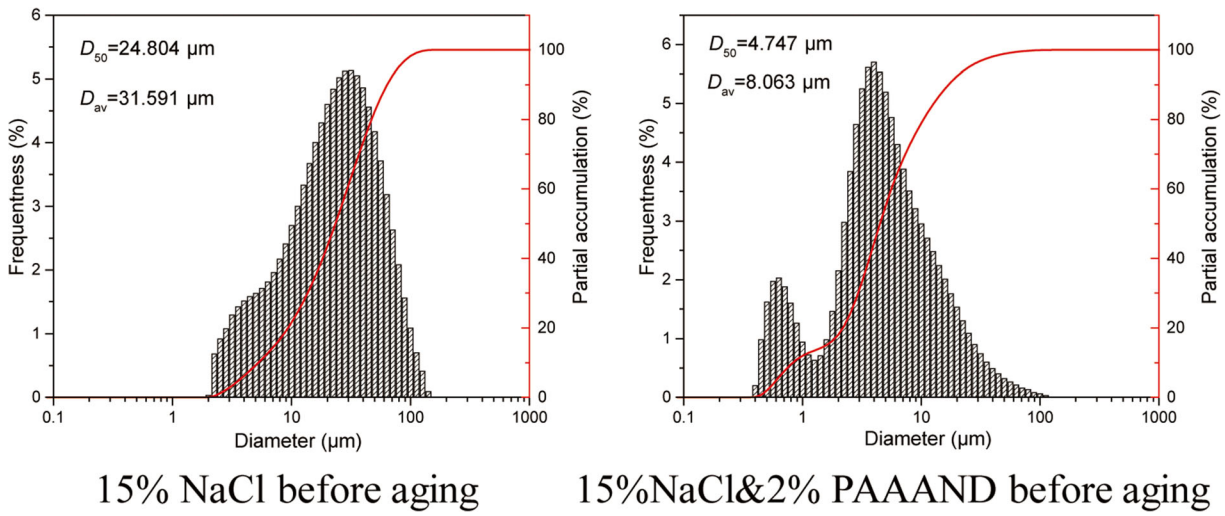

Fig. 9 Effect of PAAAND on the particle size of saltwater base slurry

decreased with aging. The presence of PAAAND increased the absolute value of the zeta potential compared to aged freshwater base mud. The PAAAND copolymer filtrate reducer, therefore, can effectively improve the zeta potential of drilling mud and prevent clay particle coalescence.

The zeta potential of saltwater drilling mud was much lower than that of freshwater mud (Fig. 13).

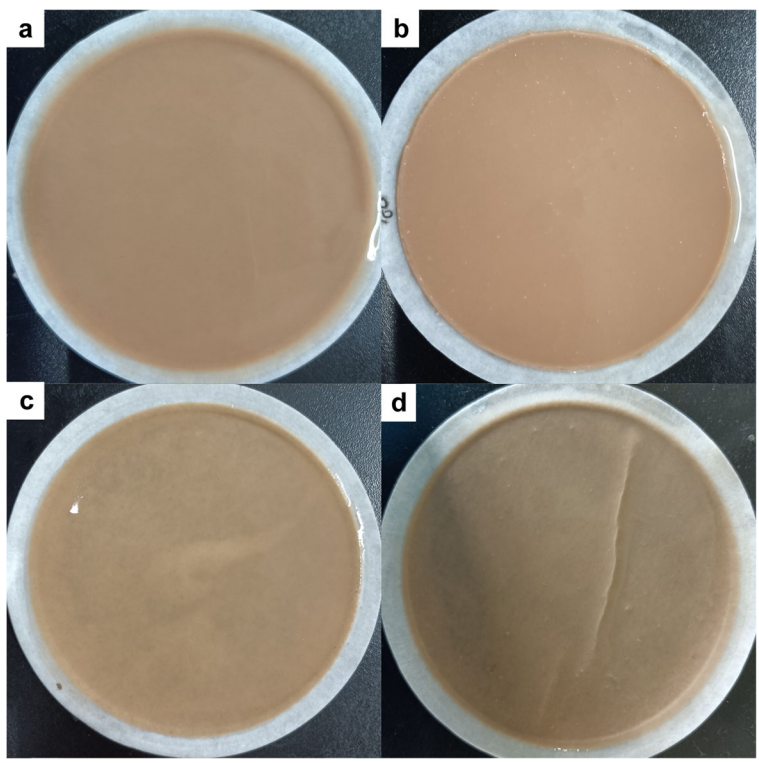

Fig. 10 **a** The base slurry filter cake before aging, **b** the base slurry filter cake after aging, **c** the 1% PAAAND base slurry filter cake before aging, and **d** the 1% PAAAND base slurry filter cake after aging

https://doi.org/10.1007/s42860-022-00181-w Published online by Cambridge University Press

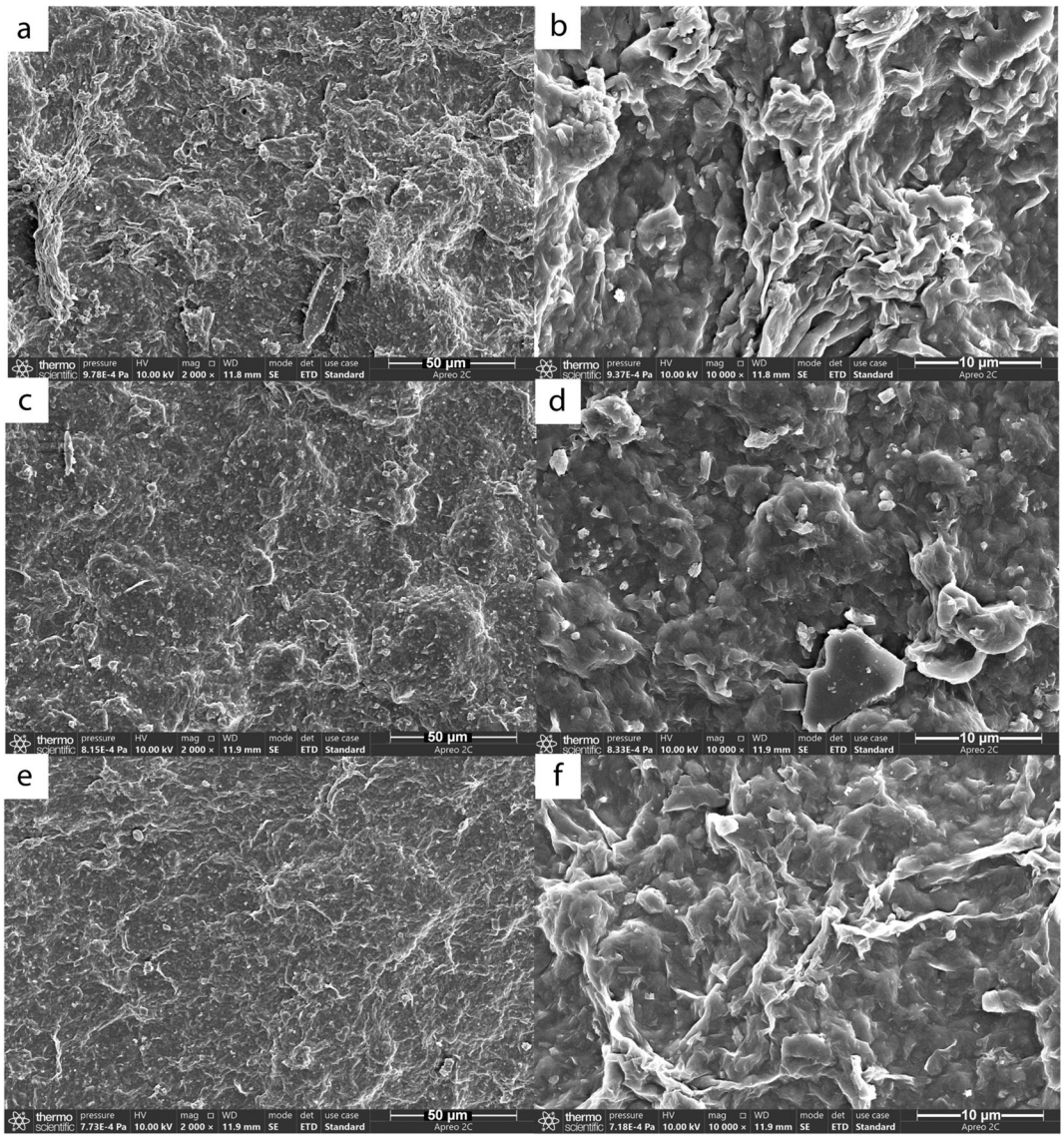

Fig. 11 **a** Base slurry before aging, **b** base slurry before aging (greater magnification), **c** 1% PAAAND base slurry before aging, **d** 1% PAAAND base slurry before aging (greater magnification), **e** 1% PAAAND base slurry after aging, and **f** 1% PAAAND base slurry after aging (greater magnification)

However, the absolute value of the zeta potential of the clay particles in the PAAAND saltwater drilling mud increased and was greater than that of freshwater base mud. The fundamental reason was that PAAAND can adsorb on the surface of the clay particles, increase the thickness of the hydration film, and then increase its zeta potential. PAAAND, thus, can protect the colloidal stability of the clay particles in saltwater drilling mud.

The Interaction Mechanism between Bentonite and Polymer The above experiments provide clarity as to the interaction mechanism between bentonite and polymer. The basal surfaces of the clay are negatively charged and the edge charge pH dependent. A PAAAND polymer chain contains sulfonic acid, carboxyl, and amide groups, and a quaternary ammonium cation. The amide group will adsorb to the hydroxyl groups at the broken Si–OH and Al–OH clay edges

https://doi.org/10.1007/s42860-022-00181-w Published online by Cambridge University Press

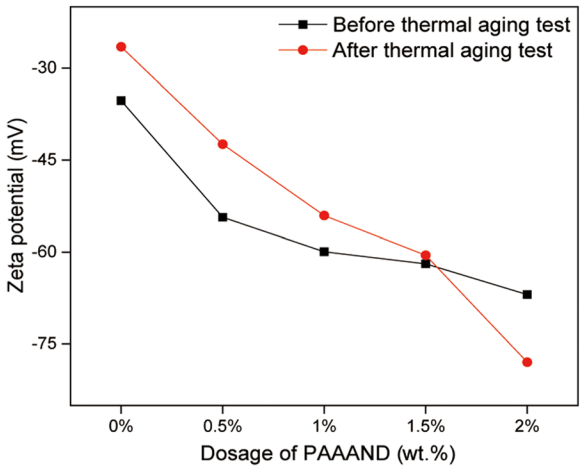

Fig. 12 Effect of PAAAND content on zeta potential of drilling mud

with a hydrogen bond. The sulfonic acid and carboxyl groups will adsorbe to the clay edges by electrostatic attraction, and the quaternary ammonium cation will adsorb to the negatively charged basal surfaces by cation exchange. When sulfonic acid and carboxyl groups were adsorbed on the surface of montmorillonite, the hydration film on the montmorillonite surface thickened, the zeta potential increased, montmorillonite dispersion increased, and the particle size decreased. The decrease in particle size corresponded well with the observed values for 0% PAAAND, 0.5% PAAAND, and 1% PAAAND (Fig. 7). However, when the amount of polymer increased to 1.5% (Fig. 7), the volume of polymer adsorbed on the clay surface increased and the particle size increased. According to the bridging theory, only small particles are not conducive to bridging and plugging, so even though the particle

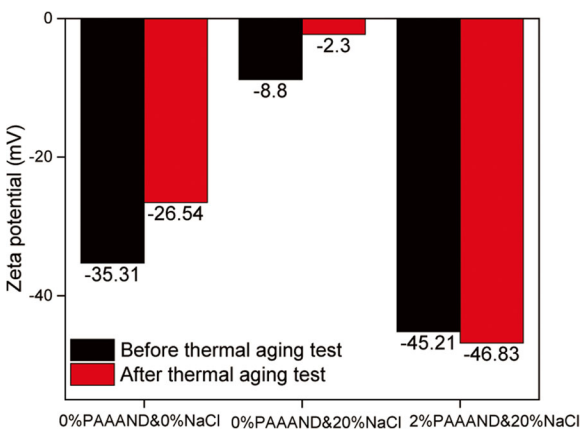

Fig. 13 Effect of salt and PAAAND on the zeta potential of drilling mud

size increased with the greater amount of polymer, the filtration rate decreased. The relationship between bentonite and polymer is illustrated simply in Fig. 14, which shows how a compact filter cake could be formed to reduce the filtration loss.

Summary and Conclusions

(1) 4-vinyl benzyl chloride, dimethylamine, and 1,3-propane sultone were used to synthesize a betaine-type zwitterionic functional monomer named DVBAPS(3-(dimethyl (4-vinyl benzyl) ammonia) propyl sulfonate), which was combined with other polymers to create the co-polymer PAAAND. The respective polymer proportions were as follows: n(AM):n(AA):n(AMPS):n(NVP):n(DVBAPS) = 30:25:35:10:5. The total mass fraction of monomers was 25%, the reaction temperature was 50°C, pH = 7, the amount of initiator was 0.4% of the mass of monomer, and the reaction time was 6 h. FTIR and ^{1}H NMR test results showed that the target polymer was successfully prepared.

(2) PAAAND resisted high temperatures to 230°C. Aging at 230°C for 16 h yielded values for FL_{API} of 8.4 mL and for FL_{HTHP} of 25.6 mL. It also is unaffected by saturated NaCl solution.

(3) Through comparative API filtration tests, PAAAND performed better in controlling the fluid loss of base slurry than that of similar commercial products Driscal-D, Dristemp, and Polydrill.

(4) After adding PAAAND to the base slurry, the bentonite layer spacing decreased from 1.548 to 1.226 nm. PAAAND also exhibited clay-expansion inhibition properties.

(5) The filtration reduction mechanism of the copolymer in drilling mud was studied by SEM, laser particle-size analysis, and zeta potential measurements. The results showed that the addition of copolymer PAAAND made the drilling fluid filter cake more compact, and the filter cake maintained its compactness under high temperatures. Particle-size analysis revealed that the particle size and average diameter of particles decreased, which improved the particle-size distribution of the drilling mud. This state was conducive to the system forming a dense filter cake structure through the close accumulation between particles to reduce the fluid loss. PAAAND can increase the absolute

https://doi.org/10.1007/s42860-022-00181-w Published online by Cambridge University Press

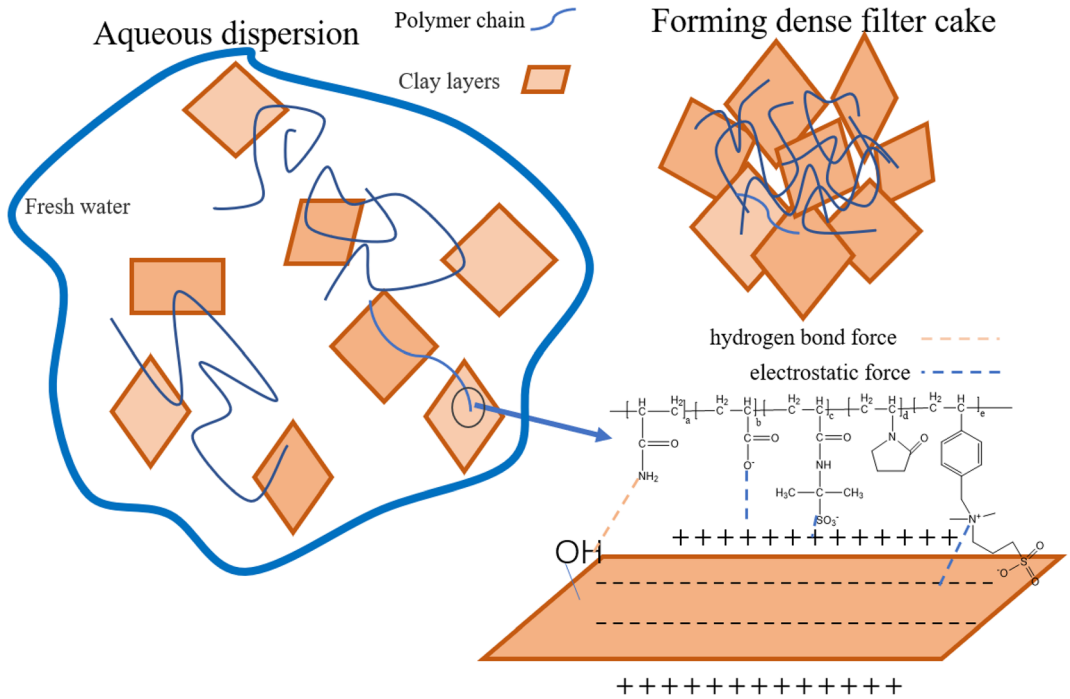

Fig. 14 Illustration of the possible interaction between bentonite and polymers

value of the zeta potential in drilling mud, which in turn improves the colloidal stability of drilling mud and reduces filtration.

Acknowledgments The authors are very grateful for the bentonite provided by Hualai Dingsheng and to tutor Lin Ling for providing the laboratory, instruments, and reagents.

Funding There is no funding for this article.

Data Availability The data that support this study are available in the article.

Declarations

Conflict of Interest There are no other relationships or activities that could appear to have influenced the submitted work. The authors declare that they have no conflict of interest. All authors agree to submit for publication.

References

Abu-Jdayil, B., & Ghannam, M. (2014). The Modification of Rheological Properties of Sodium Bentonite-water Dispersions with Low Viscosity CMC Polymer Effect. *Energy Sources Part a-Recovery Utilization and Environmental Effects, 36*(10), 1037–1048. https://doi.org/10.1080/15567036.2010.551260

Chang, X., Sun, J., Zhang, F., Lv, K., Zhou, X., Wang, J., & Zhao, J. (2020). A novel zwitterionic quaternary copolymer as a fluid-loss additive for water-based drilling fluids. *Energy Sources Part A: Recovery Utilization and Environmental Effects*, 1–14. https://doi.org/10.1080/15567036.2020.1766600

Dai, Z. W., Sun, J. S., Wang, Y., & Iop. (2019). A Polymer-based Drilling Fluid with High Temperature, Salt and Calcium Resistance Property. In *4th International Conference on Advances in Energy Resources and Environment Engineering* (Vol. 237). https://doi.org/10.1088/1755-1315/237/5/052058

De Monaco Lopes, B., Lessa, V. L., Silva, B. M., Carvalho Filho, M. A. D. S., Schnitzler, E., & Lacerda, L. G. (2015). Xanthan gum: properties, production conditions, quality and economic perspective. *Journal of Food and Nutrition Research (Bratislava, Slovakia), 54*(3), 185–194.

Gurkaynak, A., Tubert, F., Yang, J., Matyas, J., Spencer, J. L., & Gryte, C. C. (1996). High-temperature degradation of poly(-acrylic acid) in aqueous solution. *Journal of Polymer Science, Part A: Polymer Chemistry, 34*(3), 349–355. https://doi.org/10.1002/(SICI)1099-0518(199602)34:3<349::AID-POLA3>3.0.CO;2-P

Hasan, M. L., Abidin, N. A. Z., & Singh, A. (2018). The rheological performance of guar gum and castor oil as additives in water-based drilling fluid. *Materials Today-Proceedings, 5*(10), 21810–21817.

Hermansson, M. (1999). The DLVO theory in microbial adhesion. *Colloids and Surfaces, B: Biointerfaces, 14*(1-4), 105–119. https://doi.org/10.1016/S0927-7765(99)00029-6

Lee, W.-F., & Tsai, C.-C. (1994). Synthesis and solubility of the poly(sulfobetaine)s and the corresponding cationic polymers: 1. Synthesis and characterization of sulfobetaines and the corresponding cationic monomers by nuclear magnetic resonance spectra. *Polymer, 35*(10), 2210–2217. https://doi.org/10.1016/0032-3861(94)90253-4

Li, H.-M., Zhuang, J., Liu, H.-B., Feng, L., & Dong, W. (2012). Preparation and property of 2-acrylamide-2-methylpropanesulfonic acid/acrylamide/sodium styrene sulfonate as fluid loss agent for oil well cement. *Polymer Engineering & Science, 52*(2), 431–437. https://doi.org/10.1002/pen.22101

Li, Z., Pu, X., Tao, H., Liu, L., & Su, J. (2014). Synthesis and properties of acrylamide 2-acrylamido-2-methypropane sulfonic acid sodium styrene sulfonate N-vinyl pyrrolidone quadripolymer and its reduction of drilling fluid filtration at high temperature and high salinity. *Journal of Polymer Engineering, 34*(2), 125–131. https://doi.org/10.1515/polyeng-2013-0257

Liaw, D. J., & Lin, M. C. (1990). Aqueous solution properties of an ampholytic poly[3-dimethyl(acryloyloxyethyl) ammonium propane sulfonate]. *Journal of the Chinese Institute of Chemical Engineers, 21*(1), 13–20.

Lin, L., & Luo, P. (2015). Amphoteric hydrolyzed poly(acrylamide/dimethyl diallyl ammonium chloride) as a filtration reducer under high temperatures and high salinities. *Journal of Applied Polymer Science, 132*(10). https://doi.org/10.1002/app.41581

Lin, M., Li, M., Wang, Z., & Wu, Z. (2009). A Study of Thermal Stability of Linked Polymer Solution. *Journal of Dispersion Science and Technology, 30*(6), 753–756. https://doi.org/10.1080/01932690802643154

Liu, L., Pu, X., Tao, H., Deng, Q., & Luo, A. (2018). Synthesis and characterization of comb-shaped copolymer as a filtration reducer and comparison with counterparts. *RSC Advances, 8*(21), 11424–11435. https://doi.org/10.1039/c7ra13255g

Liu, F., Zhang, Z., Wang, Z., Dai, X., Chen, M., & Zhang, J. (2019). Novel lignosulfonate/N, N-dimethylacrylamide/γ-methacryloxypropyl trimethoxy silane graft copolymer as a filtration reducer for water-based drilling fluids. *Journal of Applied Polymer Science, 137*(2). https://doi.org/10.1002/app.48274

Liu, K., Du, H. S., Zheng, T., Liu, H. Y., Zhang, M., Zhang, R., Li, H. M., Xie, H. X., Zhang, X. Y., Ma, M. G., & Si, C. L. (2021). Recent advances in cellulose and its derivatives for oilfield applications. *Carbohydrate Polymers, 259*, Article 117740. https://doi.org/10.1016/j.carbpol.2021.117740

Ma, X., Zhu, Z., Shi, W., & Hu, Y. (2016). Synthesis and application of a novel betaine-type copolymer as fluid loss additive for water-based drilling fluid. *Colloid and Polymer Science, 295*(1), 53–66. https://doi.org/10.1007/s00396-016-3980-x

Mao, H., Qiu, Z., Shen, Z., & Huang, W. (2015). Hydrophobic associated polymer based silica nanoparticles composite with core–shell structure as a filtrate reducer for drilling fluid at utra-high temperature. *Journal of Petroleum Science and Engineering, 129*, 1–14. https://doi.org/10.1016/j.petrol.2015.03.003

Mao, H., Wang, W., Ma, Y., & Huang, Y. (2020). Synthesis, characterization and properties of an anionic polymer for water-based drilling fluid as an anti-high temperature and anti-salt contamination fluid loss control additive. *Polymer Bulletin, 78*, 2483–2503. https://doi:org/10.1007/s00289-020-03227-y

Murodov, M. M., Rahmanberdiev, G. R., Khalikov, M. M., Egamberdiev, E. A., Negmatova, K. C., Saidov, M. M., & Mahmudova, N. (2012). Endurance of High Molecular Weight Carboxymethyl Cellulose in Corrosive Environments. In A. Damore, L. Grassia, & D. Acierno (Eds.), *6th International Conference on Times of Polymers* (Vol. 1459, pp. 309-311). https://doi.org/10.1063/1.4738479

Pashley, R. M., & Israelachvili, J. N. (1984). DLVO and hydration forces between mica surfaces in magnesium(2+), calcium(2+), strontium(2+), and barium(2+) chloride solutions. *Journal of Colloid and Interface Science, 97*(2), 446–455. https://doi.org/10.1016/0021-9797(84)90316-3

Perricone, A. C., Enright, D. P., & Lucas, J. M. (1986). Vinyl Sulfonate Copolymers for High-Temperature Filtration Control of Water-Based Muds. *SPE Drilling Engineering, 1*(05), 358–364. https://doi.org/10.2118/13455-pa

Roux, F. X., Audebert, R., & Quivoron, C. (1973). Pyrolysis of acrylic and methylacrylic acid polymers at moderate temperatures. *European Polymer Journal, 9*(8), 815–825.

Sharma, G., Sharma, S., Kumar, A., Al-Muhtaseb, A. H., Naushad, M., Ghfar, A. A., Mola, G. T., & Stadler, F. J. (2018). Guar gum and its composites as potential materials for diverse applications: A review. *Carbohydrate Polymers, 199*, 534–545. https://doi.org/10.1016/j.carbpol.2018.07.053

Shen, H. K., Lv, K. H., Huang, X. B., Liu, J. P., Bai, Y. R., Wang, J. T., & Sun, J. S. (2020). Hydrophobic-associated polymer-based laponite nanolayered silicate composite as filtrate reducer for water-based drilling fluid at high temperature. *Journal of Applied Polymer Science, 137*(18), Article 48608. https://doi.org/10.1002/app.48608

Smith, P. S., Browne, S. V., Heinz, T. J., & Wise, W. V. (1996). Drilling Fluid Design to Prevent Formation Damage in High Permeability Quartz Arenite Sandstones. SPE Annual Technical Conference and Exhibition.

Tang, X., Yuan, B., Yang, Y. G., & Xie, Y. Q. (2016). Preparation and performance of AMPS/AA/DMAA/SA copolymer as a filtrate reducer for oil well cementing. *Journal of Applied Polymer Science, 133*(33), Article 43824. https://doi.org/10.1002/app.43824

Wang, G., Fan, H., Jiang, G., Li, W., Ye, Y., Liu, J., Kong, X., Zhong, Z., & Qian, F. (2020). Rheology and fluid loss of a polyacrylamide-based micro-gel particles in a water-based drilling fluid. *Materials Express, 10*(5), 657–662. https://doi.org/10.1166/mex.2020.1687

Xiao, S., Zhang, Y., Shen, M., Chen, F., Fan, P., Zhong, M., Ren, B., Yang, J., & Zheng, J. (2018). Structural Dependence of Salt-Responsive Polyzwitterionic Brushes with an Anti-Polyelectrolyte Effect. *Langmuir, 34*(1), 97–105. https://doi.org/10.1021/acs.langmuir.7b03667

Xiong, B., Loss, R. D., Shields, D., Pawlik, T., Hochreiter, R., Zydney, A. L., & Kumar, M. (2018). Polyacrylamide degradation and its implications in environmental systems. *NPJ*

Clean Water, 1(1), 1–9. https://doi.org/10.1038/s41545-018-0016-8

Xiping, M., Zhongxiang, Z., Daiyong, H., & Wei, S. (2017). Synthesis and performance evaluation of a water-soluble copolymer as high-performance fluid loss additive for water-based drilling fluid at high temperature. *Russian Journal of Applied Chemistry, 89*(10), 1694–1705. https://doi.org/10.1134/s1070427216100190

Yang, M.-H. (1998). The two-stages thermal degradation of polyacrylamide. *Polymer Testing, 17*(3), 191–198. https://doi.org/10.1016/S0142-9418(97)00036-6

Yang, P., Li, T. B., Wu, M. H., Zhu, X. W., & Sun, X. Q. (2015). Analysis of the effect of polyanionic cellulose on viscosity and filtrate volume in drilling fluid. *Materials Research Innovations, 19*, 12–16. https://doi.org/10.1179/1432891715z.0000000001329

Yuan, J., Zhang, D., He, X., Ni, Y., Che, L., Wu, J., Wu, B., Wang, Y., Wang, S., Sha, D., Zheng, S. Y., & Yang, J. (2021). Cationic peptide-based salt-responsive antibacterial hydrogel dressings for wound healing. *International Journal of Biological Macromolecules, 190*, 754–762. https://doi.org/10.1016/j.ijbiomac.2021.09.019

Zheng, X. H., Yang, S. W., & Lei, Z. L. (2013). Synthesis, Characterization, and Evaluation of a Fluid Loss Agent for High-Temperature Drilling Fluid. *American Laboratory, 45*(10), 22–25.

Zheng, W. L., Wu, X. M., & Huang, Y. M. (2020). Impact of polymer addition, electrolyte, clay and antioxidant on rheological properties of polymer fluid at high temperature and high pressure. *Journal of Petroleum Exploration and Production Technology, 10*(2), 663–671. https://doi.org/10.1007/s13202-019-0732-8

Zheng, S. Y., Mao, S., Yuan, J., Wang, S., He, X., Zhang, X., Du, C., Zhang, D., Wu, Z. L., & Yang, J. (2021). Molecularly Engineered Zwitterionic Hydrogels with High Toughness and Self-Healing Capacity for Soft Electronics Applications. *Chemistry of Materials, 33*(21), 8418–8429. https://doi.org/10.1021/acs.chemmater.1c02781

Zhao, Z., Pu, X., Xiao, L., Wang, G., Su, J., & He, M. (2015). Synthesis and properties of high temperature resistant and salt tolerant filtrate reducer N,N-dimethylacrylamide 2-acrylamido-2-methyl-1-propyl dimethyl diallyl ammonium chloride N-vinylpyrrolidone quadripolymer. Journal of Polymer Engineering, 35(7), 627-635. doi:10.1515/polyeng-2014-0260